

DEFAKEHOP: A LIGHT-WEIGHT HIGH-PERFORMANCE DEEPPFAKE DETECTOR

Hong-Shuo Chen¹, Mozhdeh Rouhsedaghat¹, Hamza Ghani¹, Shuowen Hu², Suyu You², C.-C. Jay Kuo¹

University of Southern California, Los Angeles, California, USA¹
Army Research Laboratory, Adelphi, Maryland, USA²

ABSTRACT

A light-weight high-performance Deepfake detection method, called DefakeHop, is proposed in this work. State-of-the-art Deepfake detection methods are built upon deep neural networks. DefakeHop extracts features automatically using the successive subspace learning (SSL) principle from various parts of face images. The features are extracted by c/w Saab transform and further processed by our feature distillation module using spatial dimension reduction and soft classification for each channel to get a more concise description of the face. Extensive experiments are conducted to demonstrate the effectiveness of the proposed DefakeHop method. With a small model size of 42,845 parameters, DefakeHop achieves state-of-the-art performance with the area under the ROC curve (AUC) of 100%, 94.95%, and 90.56% on UADFV, Celeb-DF v1 and Celeb-DF v2 datasets, respectively.

Index Terms— Light-weight, Deepfake detection, Successive subspace learning (SSL).

1. INTRODUCTION

As the number of Deepfake video contents grows rapidly, automatic Deepfake detection has received a lot of attention in the community of digital forensics. There were 7,964 Deepfake video clips online at the beginning of 2019. The number almost doubled to 14,678 in nine months. Deepfake videos can be potentially harmful to society, from non-consensual explicit content creation to forged media by foreign adversaries used in disinformation campaigns. Besides the large quantity, another major threat is that fake video quality has improved a lot over a short period of time. The rise in quality makes it increasingly difficult for humans to detect the difference between real and fake videos without a side by side comparison. As a result, an automatic and effective Deepfake detection mechanism is in urgent need. It is also desired to have a software solution that runs easily on mobile devices to provide automatic warning messages to people when fake videos are played. This is the objective of our current research.

Most state-of-the-art Deepfake detection methods are based upon deep learning (DL) technique and can be mainly categorized into two types: methods based on convolutional neural networks (CNNs) [1, 2, 3, 4, 5, 6] and methods that

integrate CNNs and recurrent neural networks (RNNs) [7, 8]. While the former focuses solely on images, the latter takes both spatial and temporal features into account. DL-based solutions have several shortcomings. First, their size is typically large containing hundreds of thousands or even millions of model parameters. Second, training them is computationally expensive. There are also non-DL-based Deepfake detection methods [9, 10, 11], where handcrafted features are extracted and fed into classifiers. The performance of non-DL-based methods is usually inferior to that of DL-based ones.

A new non-DL-based solution to Deepfake detection, called DefakeHop, is proposed in this work. DefakeHop consists of three main modules: 1) PixelHop++, 2) feature distillation and 3) ensemble classification. To derive the rich feature representation of faces, DefakeHop extracts features using PixelHop++ units [12] from various parts of face images. The theory of PixelHop++ have been developed by Kuo *et al.* using SSL [13, 14, 12]. PixelHop++ has been recently used for feature learning from low-resolution face images [15, 16] but, to the best of our knowledge, this is the first time that it is used for feature learning from patches extracted from high-resolution color face images. Since features extracted by PixelHop++ are still not concise enough for classification, we also propose an effective feature distillation module to further reduce the feature dimension and derive a more concise description of the face. Our feature distillation module uses spatial dimension reduction to remove spatial correlation in a face and a soft classifier to include semantic meaning for each channel. Using this module the feature dimension is significantly reduced and only the most important information is kept. Finally, with the ensemble of different regions and frames, DefakeHop achieves state-of-the-art results on various benchmarks.

The rest of this paper is organized as follows. Background is reviewed in Sec. 2. The proposed DefakeHop method is presented in Sec. 3. Experiments are given in Sec. 4 to demonstrate the effectiveness. Finally, conclusion is pointed out in Sec. 5.

2. BACKGROUND REVIEW

2.1. Non-DL-based Methods

Yang *et al.* [9] exploited discrepancy between head poses and facial landmarks for Deepfake detection. They first extracted

features such as rotational and translational differences between real and fake videos and then applied the SVM classifier. Agarwal *et al.* [10] focused on detecting Deepfake video of high-profile politicians and leveraged specific facial patterns of individuals when they talk. They used the one-class SVM, which is only trained on real videos of high profile individuals. Matern *et al.* [11] used landmarks to find visual artifacts in fake videos, e.g., missing reflections in eyes, teeth replaced by a single white blob, etc. They adopted the logistic regression and the multi-layer perceptron (MLP) classifiers.

2.2. DL-based Methods

CNN Solutions. Li *et al.* [17] used CNNs to detect the warping artifact that occurs when a source face is warped into the target one. Several well known CNN architectures such as VGG16, ResNet50, ResNet101, and ResNet152 were tried. VGG16 was trained from scratch while ResNet models were pretrained on the ImageNet dataset and fine-tuned by image frames from Deepfake videos. Afchar *et al.* [4] proposed a mesoscopic approach to Deepfake detection and designed a small network that contains only 27,977 trainable parameters. Tolosana *et al.* [1] examined different facial regions and landmarks such as eyes, nose, mouth, the whole face, and the face without eyes, nose, and mouth. They applied the Xception network to each region and classify whether it is fake or not.

Integrated CNN/RNN Solutions. The integrated CNN/RNN solutions exploit both spatial and temporal features. Sabir *et al.* [8] applied the DenseNet and the bidirectional RNN to aligned faces. Güera and Delp [7] first extracted features from a fully-connected-layer removed InceptionV3, which was trained on the ImageNet. Then, they fed these features to an LSTM (Long short-term memory) for sequence processing. Afterward, they mapped the output of the LSTM, called the sequence descriptor, to a shallow detection network to yield the probability of being a fake one.

3. DEFAKEHOP METHOD

Besides the face image preprocessing step (see Fig. 1), the proposed DefakeHop method consists of three main modules: 1) PixelHop++ 2) feature distillation and 3) ensemble classification. The block diagram of the DefakeHop method is shown in Fig. 2. Each of the components is elaborated below.

3.1. Face Image Preprocessing

Face image preprocessing is the initial step in the DefakeHop system. As shown in Fig. 1, we crop out face images from video frames and then align and normalize the cropped-out faces to ensure proper and consistent inputs are fed to the following modules in the pipeline. Preprocessing allows DefakeHop to handle different resolutions, frame rates, and postures. Some details are given below. First, image frames

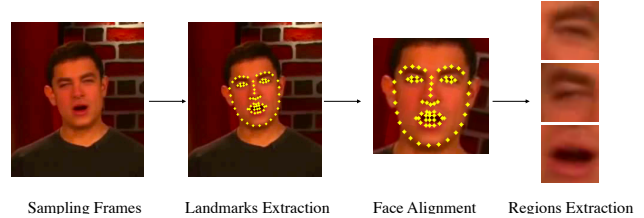


Fig. 1. Face image preprocessing.

are sampled from videos. Then, 68 facial landmarks are extracted from each frame by using an open-source toolbox “OpenFace2” [18]. After extracting facial landmarks from a frame, faces are resized to 128×128 and rotated to specific coordinates to make all samples consistent without different head poses or face sizes. Finally, patches of size 32×32 are cropped from different parts of the face (e.g., the left eye, right eye and mouth) as the input data to PixelHop++ module.

3.2. PixelHop++ Module

PixelHop++ extracts rich and discriminant features from local blocks. As shown in Fig. 2, the input is a color image of spatial resolution 32×32 that focuses on a particular part of a human face. The block size and stride are hyperparameters for users to decide. This process can be conducted in multiple stages to get a larger receptive field. The proposed DefakeHop system has three PixelHop++ units in cascade, each of which has a block size of 3×3 with the stride equal to one without padding. The block of a pixel of the first hop contains $3 \times 3 \times K_0 = 9K_0$ variables as a flattened vector, where $K_0 = 3$ for the RGB input.

Spectral filtering and dimension reduction. We exploit the statistical correlations between pixel-based neighborhoods and apply the *c/w* Saab transform to the flattened vector of dimension $K_1 = 9K_0 = 27$ to obtain a feature representation of dimension K_{11} (see discussion in Sec. 3.3).

Spatial max-pooling. Since the blocks of two adjacent pixels overlap with each other, there exists spatial redundancy between them. We conduct the (2×2) -to- (1×1) maximum pooling unit to reduce the spatial resolution of the output furthermore.

3.2.1. Channel-wise (*c/w*) Saab Transform

The Saab (subspace approximation via adjusted bias) transform [14] is a variant of PCA. It first decomposes a signal space into the local mean and the frequency components and then applies the PCA to the frequency components to derive kernels. Each kernel represents a certain frequency-selective filter. A kernel of a larger eigenvalue extracts a lower frequency component while a kernel of a smaller eigenvalue extracts a higher frequency component. The high-frequency

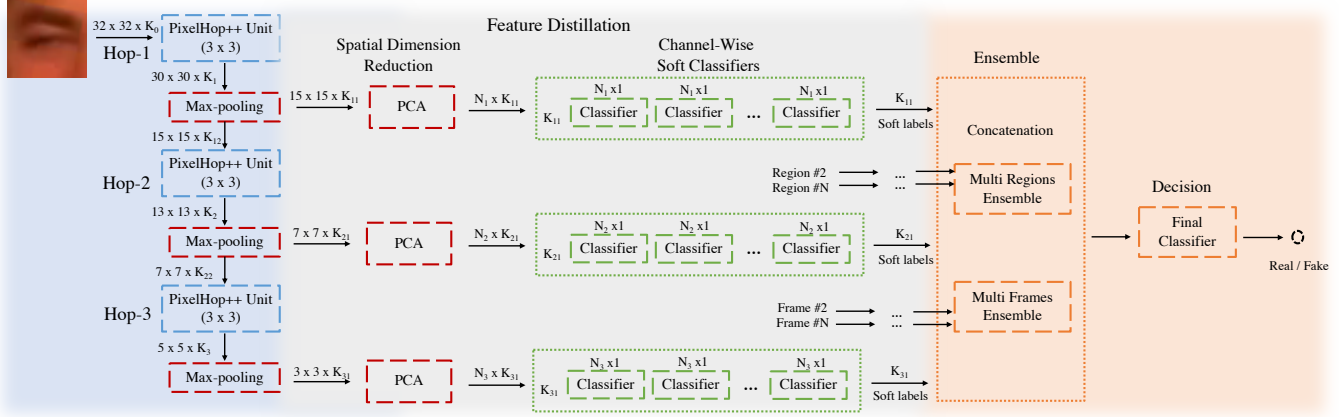


Fig. 2. An overview of the DefakeHop method.

components with very small eigenvalues can be discarded for dimension reduction.

This scheme can be explained by the diagram in Fig. 3, where a three-stage *c/w* Saab transform is illustrated. By following the system in Fig. 2, the root of the tree is the color image of dimension $32 \times 32 \times 3$. The local input vector to the first hop has a dimension of $3 \times 3 \times 3 = 27$. Thus, we can get a local mean and 26 frequency components. We divide them into three groups: low-frequency channels (in blue), mid-frequency channels (in green), and high-frequency channels (in gray). Each channel can be represented as a node in the tree. Responses of high-frequency channels can be discarded, responses of mid-frequency channels are kept, yet no further transform is performed due to weak spatial correlations, and responses of low-frequency channels will be fed into the next stage for another *c/w* Saab transform due to stronger spatial correlations. Responses in Hop-1, Hop-2 and Hop-3 are joint spatial-spectral representations. The first few hops contain more spatial detail but have a narrower view. As the hop goes deeper, it has less spatial detail but with a broader view. The channel-wise (*c/w*) Saab transform exploits channel separability to reduce the model size of the Saab transform without performance degradation.

3.3. Feature Distillation Module

After feature extraction by PixelHop++, we derive a small and effective set of features of a face. However, the output dimension of PixelHop++ is still not concise enough to be fed into a classifier. For example, the output dimension of the first hop is $15 \times 15 \times K_{11} = 225K_{11}$. We use two methods to further distill the feature to get a compact description of a face being fake or real.

Spatial dimension reduction Since input images are face patches from the same part of human faces, there exist strong correlations between the spatial responses of 15×15 for a given channel. Thus, we apply PCA for further spatial di-

dimension reduction. By keeping the top N_1 PCA components which contain about 90% of the energy of the input images, we get a compact representation of $N_1 \times K_{11}$ dimension.

Channel-wise Soft Classification After removing spatial and spectral redundancies, we obtain K_{11} channels from each hop with a rather small spatial dimension N_1 . For each channel, we train a soft binary classifier to include the semantic meaning. The soft decision provides the probability of a specific channel being related to a fake video. Different classifiers could be used here in different situations. In our model, the extreme gradient boosting classifier (XGBoost) is selected because it has a reasonable model size and is efficient to train to get a high AUC. The max-depth of XGBoost is set to one for all soft classifiers to prevent overfitting.

For each face patch, we concatenate the probabilities of all channels to get a description representing the patch. The output dimension becomes K_{11} , which is reduced by a large amount comparing to the output of PixelHop++. It will be fed into a final classifier to determine the probability of being fake for this face patch.

3.4. Ensemble Classification Module

We integrate soft decisions from all facial regions (different face patches) and selected frames to offer the final decision whether a video clip is fake or real according to the following procedure.

Multi-Region Ensemble. Since each facial region might have different strength and weakness against different Deepfake manipulations [1], we concatenate the probabilities of different regions together. In experiments reported in Sec. 4, we focus on three facial regions. They are the left eye, the right eye, and the mouth.

Multi-Frame Ensemble. Besides concatenating different regions, for each frame, we concatenate the current frame and its adjacent 6 frames (namely, 3 frames before and 3 frames after) so as to incorporate the temporal information.

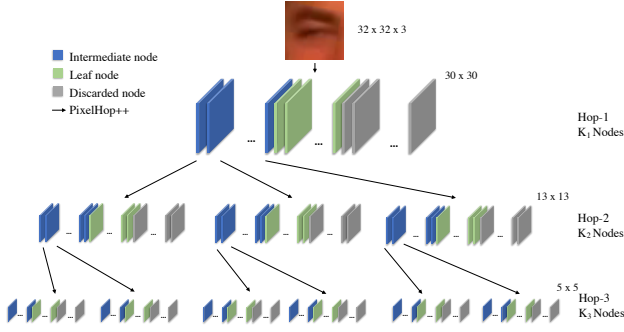


Fig. 3. Illustration of the *c/w* Saab transform.

Finally, for the whole video clip, we compute its probability of being fake by averaging the probabilities of all frames from the same video. Different approaches to aggregate frame-level probabilities can be used to determine the final decision.

4. EXPERIMENTS

We evaluate the performance of DefakeHop on four Deepfake video datasets: UADFV, FaceForensics++ (FF++), Celeb-DF v1, and Celeb-DF v2, and compare the results with state-of-the-art Deepfake detection methods. UADFV does not specify the train/test split. We randomly select 80% for training and 20% for testing. FF++ and Celeb-DF provide the test set, and all other videos are used for training the model.

Benchmarking Datasets. Deepfake video datasets are categorized into two generations based on the dataset size and Deepfake methods used. The first generation includes UADFV and FF++. The second generation includes Celeb-DF version 1 and version 2. Fake videos of the second generation are more realistic, which makes their detection more challenging.

Table 1. The AUC value for each facial region and the final ensemble result.

	Left eye	Right eye	Mouth	Ensemble
UADFV	100%	100%	100%	100%
FF++ / DF	94.37%	93.73%	94.25%	97.45%
Celeb-DF v1	89.69%	88.20%	92.66%	94.95%
Celeb-DF v2	85.17%	86.41%	89.66%	90.56%

4.1. Detection Performance

DefakeHop is benchmarked with several other methods using the area under the ROC curve (AUC) metric in Table 2. We report both frame-level and video-level AUC values for DefakeHop. For the frame-level AUC, we follow the evaluation done in [20] that considers key frames only (rather than all frames).

DefakeHop achieves the best performance on UADFV, Celeb-DF v1, and Celeb-DF v2 among all methods. On FF++/DF, its AUC is only 2.15% lower than the best result ever reported. DefakeHop outperforms other non-DL methods [9, 11] by a significant margin. It is also competitive against DL methods [1, 6, 5, 2]. The ROC curve of DefakeHop with respect to different datasets is shown in Fig. 4.

We compare the detection performance by considering different factors.

Facial Regions The performance of DefakeHop with respect to different facial regions and their ensemble results are shown in Table 1. The ensemble of multiple facial regions can boost the AUC values by up to 5%. Each facial region has different strengths on various faces, and their ensemble gives the best result.

Video Quality. In the experiment, we focus on compressed videos since they are challenging for Deepfake detection algorithms. We evaluate the AUC performance of DefakeHop on videos with different qualities in Table 3. As shown in the table, the performance of DefakeHop degrades by 5% as video quality becomes worse. Thus, DefakeHop can reasonably handle videos with different qualities.

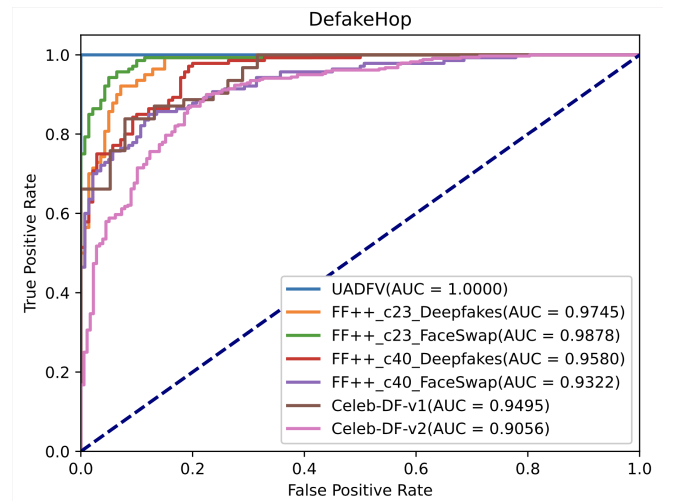


Fig. 4. The ROC curve of DefakeHop for different datasets.

4.2. Model Size Computation

PixelHop++ units Filters in all three hops have a size of 3x3. The maximum number of PixelHop++ units is limited to 10. For Hop-1, the input has three channels, leading to a 27D input vector. For Hop-2 and Hop-3, since we use the channel-wise method, each input has only 1 channel, leading to a 9D input vector. There are multiple *c/w* Saab transforms for Hop-2 and Hop-3. The channel would be selected across multiple *c/w* Saab transforms. Therefore, it is possible to get more than 9 channels for Hop-2 and Hop-3. At most 27×10 , 9×10 , 9×10 parameters are used in 3 PixelHop++ units.

Table 2. Comparison of the detection performance of benchmarking methods with the AUC value at the frame level as the evaluation metric. The **boldface** and the underbar indicate the best and the second-best results, respectively. The *italics* means it does not specify frame or video level AUC. The AUC results of DefakeHop is reported in both frame-level and video-level. The AUC results of benchmarking methods are taken from [19] and [20]. ^a deep learning method, ^b non deep learning method.

	Method	1st Generation datasets		2nd Generation datasets		Number of parameters
		UADFV	FF++ / DF	Celeb-DF v1	Celeb-DF v2	
Zhou <i>et al.</i> (2017) [3]	InceptionV3 ^a	85.1%	70.1%	55.7%	53.8%	24M
Afchar <i>et al.</i> (2018) [4]	Meso4 ^a	84.3%	84.7%	53.6%	54.8%	27.9K
Li <i>et al.</i> (2018) [17]	FWA ^a (ResNet-50)	97.4%	80.1	53.8%	56.9%	23.8M
Yang <i>et al.</i> (2019) [9]	HeadPose ^b (SVM)	89%	47.3%	54.8%	54.6%	-
Matern <i>et al.</i> (2019) [11]	VA-MLP ^b	70.2%	66.4%	48.8%	55%	-
Rosler <i>et al.</i> (2019) [2]	Xception-raw ^a	80.4%	99.7%	38.7%	48.2%	22.8M
Nguyen <i>et al.</i> (2019) [5]	Multi-task ^a	65.8%	76.3%	36.5%	54.3%	-
Nguyen <i>et al.</i> (2019) [6]	CapsuleNet ^a	61.3%	96.6%	-	57.5%	3.9M
Sabir <i>et al.</i> (2019) [8]	<i>DenseNet+RNN</i> ^a	-	<u>99.6%</u>	-	-	25.6M
Li <i>et al.</i> (2020) [17]	DSP-FWA ^a (SPPNet)	<u>97.7%</u>	93%	-	64.6%	-
Tolosana <i>et al.</i> (2020) [1]	<i>Xception</i> ^a	100%	99.4%	83.6%	-	22.8M
Ours	DefakeHop (Frame)	100%	95.95%	<u>93.12%</u>	<u>87.65%</u>	42.8K
	DefakeHop (Video)	100%	97.45%	94.95%	90.56%	42.8K

Table 3. Comparison of Deepfake algorithms and qualities.

	FF++ with Deepfakes		FF++ with FaceSwap	
	HQ (c23)	LQ (c40)	HQ (c23)	LQ (c40)
Frame	95.95%	93.01%	97.87%	89.14%
Video	97.45%	95.80%	98.78%	93.22%

Spatial PCA Hop-1 is reduced from 225 to 45, Hop-2 is reduced from 49 to 30, and Hop-3 is reduced from 9 to 5. The number of parameters for spatial PCAs are 225×45 , 49×25 , and 9×5 . The number of kept channels 45, 25, 5 is selected based on keeping about 90% of energy.

XGBoost The number of trees is set to 100. Each tree includes intermediate and leaf nodes. Intermediate nodes decide the dimension and boundary to split (i.e., 2 parameters per node) while the leaf nodes determine the predicted value (i.e., 1 parameter per node). When the max-depths are 1 and 6, the number of parameters are 400 and 19,000. The max-depth of channel-wise and ensemble XGBoosts are set to 1 and 6, respectively. Thus, the total number of parameters for 30 channel-wise XGBoosts is 12,000 and the number of parameters of the ensemble XGBoost is 19,000.

The above calculations are summarized in Table 4. The final model size, 42,845, is actually an upper-bound estimate since the maximum depth in the XGBoost and the maximum channel number per hop are upper bounded.

Train on a small data size We observe that DefakeHop demands fewer training videos. An example is given to illustrate this point. Celeb-DF v2 has 6011 training videos in total.

Table 4. The number of parameters for various parts.

Subsystem	Number of Parameters
Pixelhop++ Hop-1	270
Pixelhop++ Hop-2	90
Pixelhop++ Hop-3	90
PCA Hop-1	10,125
PCA Hop-2	1,225
PCA Hop-3	45
Channel-Wise XGBoost(s)	12,000
Fianl XGBoost	19,000
Total	42,845

We train DefakeHop with a randomly increasing video number in three facial regions and see that DefakeHop can achieve nearly 90% AUC with only 1424 videos (23.6% of the whole dataset). In Fig. 5 the AUC of test videos is plotted as a function of the number of training videos of Celeb-DF v2. As shown in the figure, DefakeHop can achieve about 85% AUC with less than 5% (250 videos) of the whole training data.

5. CONCLUSION

A light-weight high-performance method for Deepfake detection, called DefakeHop, was proposed. It has several advantages: a smaller model size, fast training procedure, high detection AUC and needs fewer training samples. Extensive experiments were conducted to demonstrate its high detection performance.

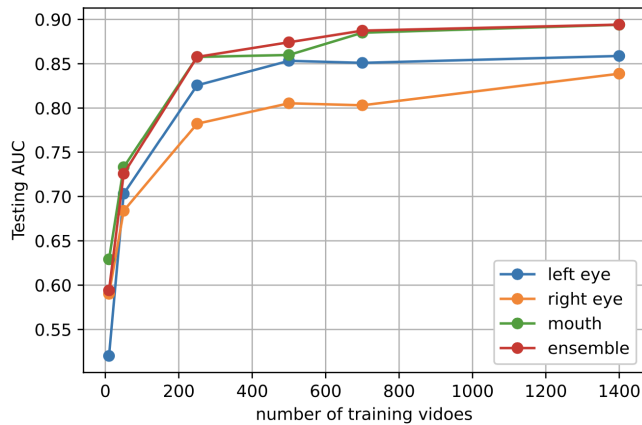


Fig. 5. The plot of AUC values as a function of the training video number.

6. REFERENCES

- [1] Ruben Tolosana, Sergio Romero-Tapiador, Julian Fierrez, and Ruben Vera-Rodriguez, “Deepfakes evolution: Analysis of facial regions and fake detection performance,” *arXiv preprint arXiv:2004.07532*, 2020.
- [2] Andreas Rossler, Davide Cozzolino, Luisa Verdoliva, Christian Riess, Justus Thies, and Matthias Nießner, “Faceforensics++: Learning to detect manipulated facial images,” in *Proceedings of the IEEE International Conference on Computer Vision*, 2019, pp. 1–11.
- [3] Peng Zhou, Xintong Han, Vlad I Morariu, and Larry S Davis, “Two-stream neural networks for tampered face detection,” in *2017 IEEE Conference on Computer Vision and Pattern Recognition Workshops (CVPRW)*. IEEE, 2017, pp. 1831–1839.
- [4] Darius Afchar, Vincent Nozick, Junichi Yamagishi, and Isao Echizen, “Mesonet: a compact facial video forgery detection network,” in *2018 IEEE International Workshop on Information Forensics and Security (WIFS)*. IEEE, 2018, pp. 1–7.
- [5] Huy H Nguyen, Fuming Fang, Junichi Yamagishi, and Isao Echizen, “Multi-task learning for detecting and segmenting manipulated facial images and videos,” *arXiv preprint arXiv:1906.06876*, 2019.
- [6] Huy H Nguyen, Junichi Yamagishi, and Isao Echizen, “Use of a capsule network to detect fake images and videos,” *arXiv preprint arXiv:1910.12467*, 2019.
- [7] David Güera and Edward J Delp, “Deepfake video detection using recurrent neural networks,” in *2018 15th IEEE International Conference on Advanced Video and Signal Based Surveillance (AVSS)*. IEEE, 2018, pp. 1–6.
- [8] Ekraam Sabir, Jiaxin Cheng, Ayush Jaiswal, Wael AbdAlmageed, Iacopo Masi, and Prem Natarajan, “Recurrent convolutional strategies for face manipulation detection in videos,” *Interfaces (GUI)*, vol. 3, no. 1, 2019.
- [9] Xin Yang, Yuezun Li, and Siwei Lyu, “Exposing deep fakes using inconsistent head poses,” in *ICASSP 2019-2019 IEEE International Conference on Acoustics, Speech and Signal Processing (ICASSP)*. IEEE, 2019, pp. 8261–8265.
- [10] Shruti Agarwal, Hany Farid, Yuming Gu, Mingming He, Koki Nagano, and Hao Li, “Protecting world leaders against deep fakes,” in *CVPR Workshops*, 2019, pp. 38–45.
- [11] Falko Matern, Christian Riess, and Marc Stamminger, “Exploiting visual artifacts to expose deepfakes and face manipulations,” in *2019 IEEE Winter Applications of Computer Vision Workshops (WACVW)*. IEEE, 2019, pp. 83–92.
- [12] Yueru Chen, Mozhdeh Rouhsedaghat, Suyu You, Raghuvver Rao, and C-C Jay Kuo, “Pixelhop++: A small successive-subspace-learning-based (ssl-based) model for image classification,” *arXiv preprint arXiv:2002.03141*, 2020.
- [13] C-C Jay Kuo, “Understanding convolutional neural networks with a mathematical model,” *Journal of Visual Communication and Image Representation*, vol. 41, pp. 406–413, 2016.
- [14] C-C Jay Kuo, Min Zhang, Siyang Li, Jiali Duan, and Yueru Chen, “Interpretable convolutional neural networks via feedforward design,” *Journal of Visual Communication and Image Representation*, vol. 60, pp. 346–359, 2019.
- [15] Mozhdeh Rouhsedaghat, Yifan Wang, Xiou Ge, Shuowen Hu, Suyu You, and C-C Jay Kuo, “Facehop: A light-weight low-resolution face gender classification method,” *arXiv preprint arXiv:2007.09510*, 2020.
- [16] Mozhdeh Rouhsedaghat, Yifan Wang, Shuowen Hu, Suyu You, and C-C Jay Kuo, “Low-resolution face recognition in resource-constrained environments,” *arXiv preprint arXiv:2011.11674*, 2020.
- [17] Yuezun Li and Siwei Lyu, “Exposing deepfake videos by detecting face warping artifacts,” in *IEEE Conference on Computer Vision and Pattern Recognition Workshops (CVPRW)*, 2019.
- [18] Tadas Baltrusaitis, Amir Zadeh, Yao Chong Lim, and Louis-Philippe Morency, “Openface 2.0: Facial behavior analysis toolkit,” in *2018 13th IEEE International Conference on Automatic Face & Gesture Recognition (FG 2018)*. IEEE, 2018, pp. 59–66.
- [19] Ruben Tolosana, Ruben Vera-Rodriguez, Julian Fierrez, Aythami Morales, and Javier Ortega-Garcia, “Deepfakes and beyond: A survey of face manipulation and fake detection,” *arXiv preprint arXiv:2001.00179*, 2020.
- [20] Yuezun Li, Xin Yang, Pu Sun, Honggang Qi, and Siwei Lyu, “Celeb-df: A large-scale challenging dataset for deepfake forensics,” in *Proceedings of the IEEE/CVF Conference on Computer Vision and Pattern Recognition*, 2020, pp. 3207–3216.